

Micellar Lyotropic Nematic Gels

Sonja Dieterich, Friedrich Stemmler, Natalie Preisig, and Frank Giesselmann*

Lyotropic liquid crystal (LLC) gels are a new class of liquid crystal (LC) networks that combine the anisotropy of micellar LLCs with the mechanical stability of a gel. However, so far, only micellar LLC gels with lamellar and hexagonal structures have been obtained by the addition of gelators to LLCs. Here, the first examples of lyotropic nematic gels are presented. The key to obtain these nematic gels is the use of gelators that have a non-amphiphilic molecular structure and thus leave the size and shape of the micellar aggregates essentially unchanged. By adding these gelators to lyotropic nematic phases, an easy and reproducible way to obtain large amounts of lyotropic nematic gels is established. These nematic gels preserve the long-range orientational order and optical birefringence of a lyotropic nematic phase but have the mechanical stability of a gel. LLC nematic gels are promising new materials for elastic and anisotropic hydrogels to be applied as water-based stimuli-responsive actuators and sensors.

The coupling of orientational order and macroscopic shape^[1,2] is the striking feature of liquid crystalline networks, such as liquid-crystalline elastomers^[3–5] (LCEs) and LC gels (LCGs).^[6–8] Today, thermotropic LCEs and LCGs are the backbone of the rapidly emerging field of soft robotics and biomimetic actuation.^[9–14] External stimuli (e.g., temperature, light) modify or destroy the LC orientational order leading to macroscopic shape changes. Drawbacks of LCEs are their often complicated and expensive fabrication as well as the limitation in the choice of external stimuli. In contrast, lyotropic liquid crystal (LLC) physical gels, which are the lyotropic counterpart to thermotropic LCEs and LCGs, are comparatively easy in fabrication and compatible to aqueous systems. Thus, they might find biomedical applications (e.g., artificial tissues) and respond to a broad range of biological and chemical stimuli such as pH-value, salt concentration, solutes, vapor pressure, and temperature, as it was shown for anisotropic hydrogels.^[15–26] LLC gels are a new approach to anisotropic hydrogels: instead of a water-swollen polymer network, a genuine LLC phase formed by micelles is

gelled by low-molecular-weight gelators (LMWGs).^[27–30] Via physical interactions, such as π - π interactions and hydrogen bonds, LMWGs form self-assembled 3D fibrillar networks (SAFINs), which arrest the fluidity of the LLC phase as a result of the gelation. The anisotropy of the LLC is thus combined with the elasticity of a gel network enabling potential applications where some mechanical stability is needed such as stimuli-responsive actuation,^[22,24,31] transdermal drug delivery^[32,33] as well as non-fluid templates for the synthesis of macroscopically aligned nanostructured materials.^[34,35]

In recent years few studies on LLC gels as a new kind of LC networks were presented.^[36–40] It was shown that the anisotropic order of the surfactant-based LLCs


is combined with the mechanical stability and elasticity of a 3D physical gel network. Lyotropic lamellar and hexagonal phases were successfully gelled by LMWGs, but so far no lyotropic nematic physical gel was obtained. In comparison to lamellar and hexagonal lyotropics, lyotropic nematic phases are less common. In recent years however the understanding of their stability has been much improved and, as a result, the pool of lyotropic nematic systems was significantly enlarged by the work of Akpınar et al.^[41–43]

Nematics are the structurally simplest LC phase due to the absence of any long-range translational order, which is also the reason for their low viscosity enabling easy alignment of lyotropic nematics before gelation. This makes lyotropic nematic gels essential for demonstrating fundamental principles in LLC gels and straightforward for the application in stimuli-responsive actuators. In a former paper we showed that lyotropic nematic physical gels are not as easily achievable as lamellar gels since the used gelator 12-HOA acts partly as cosurfactant and thus gelation of nematic LLCs with 12-HOA lead to lamellar gels only.^[40]

In this paper we restrict the term lyotropic nematic gels to the genuine nematic LLC phases formed by rod- or disk-like micelles and gelled by a fibrillar network. Please note that the term lyotropic nematic gel is also used in other contexts where the building blocks of the nematic phase are interacting with each other so that they form a gel network. This was for instance found for orientationally ordered dispersions of rigid fibers,^[44,45] nanoparticles,^[46] inverse micelles,^[47] or (bio)polymers^[48,49] in either water or organic solvents.

Here, we present the first examples of gelator-based micellar lyotropic nematic networks. We gelled the nematic N_d and N_c phases of the two surfactant systems H_2O -*n*-decanol-sodium dodecyl sulfate (SDS) and H_2O -*n*-decanol-*N,N*-dimethyl-*N*-ethylhexadecylammonium bromide (CDEAB) with the three

S. Dieterich, F. Stemmler, Dr. N. Preisig, Prof. F. Giesselmann
Institute of Physical Chemistry
University of Stuttgart
Pfaffenwaldring 55, 70569 Stuttgart, Germany
E-mail: frank.giesselmann@ipc.uni-stuttgart.de

 The ORCID identification number(s) for the author(s) of this article can be found under <https://doi.org/10.1002/adma.202007340>.

© 2021 The Authors. Advanced Materials published by Wiley-VCH GmbH. This is an open access article under the terms of the Creative Commons Attribution-NonCommercial License, which permits use, distribution and reproduction in any medium, provided the original work is properly cited and is not used for commercial purposes.

DOI: 10.1002/adma.202007340

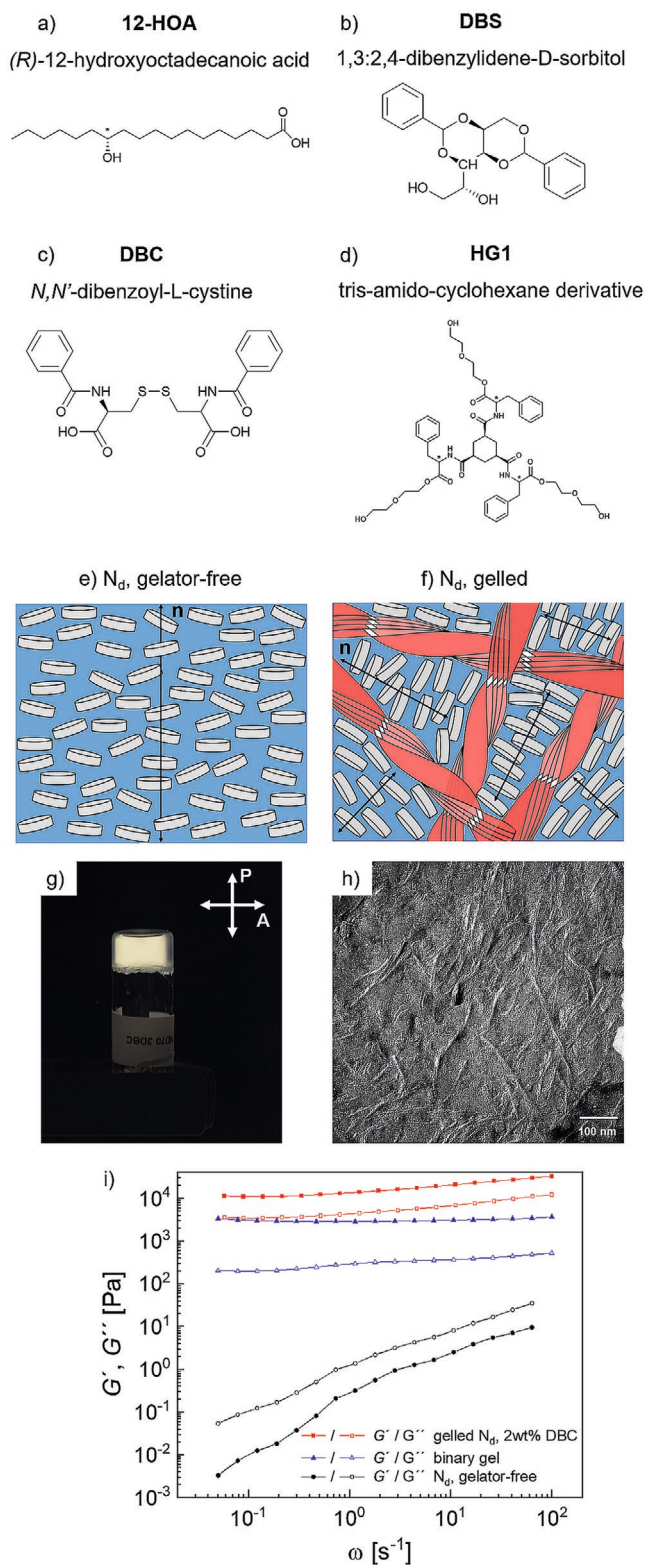


Figure 1. a–d) Molecular structure of the used LMWGs 12-HOA (a), DBS (b), DBC (c), and HG1 (d). While 12-HOA has an amphiphilic structure, the molecular structure of the other gelators is bulky, thus an incorporation of gelator molecules into the micelles is not possible for DBS, DBC, and HG1. e, f) Schematic drawings of the structure of a fluid gelator-free N_d phase (e) and the proposed structure of a gelled N_d phase (f),

low-molecular-weight gelators DBS, DBC, and HG1 (see molecular structures in **Figure 1**). Gels were achieved for all combinations with the exception of the nematic phases of the system H_2O –*n*-decanol–CDEAB with the gelator DBC. All obtained gels were nematic with the exception of the system H_2O –*n*-decanol–SDS gelled with HG1, where starting from the N_c phase an isotropic gel was received. All in all, we were able to obtain nine different lyotropic nematic gels, which are to the best of our knowledge the first examples of this new kind of water-based micellar LC networks. A complete overview on our experiments to obtain lyotropic nematic gels with these surfactant systems and gelators is found in Table S1 in the Supporting Information.

As a representative example, we will now discuss the properties of lyotropic nematic gels using the N_d phase of the surfactant system H_2O –*n*-decanol–SDS transferred into the gelled state by the gelators DBS, DBC and HG1, and make a comparison to previous results obtained with the gelator 12-HOA.^[40]

A schematic drawing of a lyotropic N_d phase and its gelled state is shown in **Figure 1e,f**, respectively. For the nematic gel, the observed sol–gel transition temperature $T_{sol-gel}$ lies above the nematic clearing temperature (the same is true for all obtained nematic gels, see Table S2, Supporting Information). Thus, in the absence of external influences, a random gel fiber network is formed upon cooling. As in the case of thermotropic nematic gels,^[8] the gel fibers probably serve as a soft template for the nematic phase leading to a nematic polydomain structure. **Figure 1g** demonstrates that the lyotropic nematic gel combines the anisotropic properties of a nematic phase with the mechanical stability of a gel since an upside down sample between crossed polarizers shows optical birefringence and no flow. A freeze-fracture electron microscopy image of the same sample reveals the gel fiber network, where twisted gel fibers with a diameter of 8–12 nm run arbitrarily through the nematic phase. The rheological measurements (**Figure 1i**) clearly reveal the solid-like elastic behavior of the nematic gel. Similar to what is observed in the binary gel, the storage modulus G' exceeds the loss modulus G'' over the full frequency range from $\omega = 0.05$ to 100 s^{-1} . This is in clear contrast to the fluid-like behavior of the gelator-free nematic phase with $G'' > G'$ and both moduli at least three orders of magnitude smaller than in the nematic gel.

The molecular structure of the used LMWGs (see **Figure 1c–f**) shows a distinct difference between that of 12-HOA and the other gelators. While DBS, DBC, and HG1 are bulky, 12-HOA has a typical amphiphilic structure with a long hydrophobic alkyl chain and a polar head group. As reported before^[40] and shown in **Figure 2** the molecular structure of 12-HOA

with n being the director. In the nematic gel, the micellar lyotropic nematic phase coexists with the gel fiber network. g, h) Gel formation is confirmed since no flow is observed when turning the sample (N_d phase with 3 wt% DBC) upside down, but the nematic gel shows optical birefringence between crossed polarizers (g) and the gel fibers are visible in electron microscopy images (h). An example is shown for the N_c phase gelled with 2 wt% DBC. i) Storage modulus G' (filled symbols) and loss modulus G'' (open symbols) for the gelator-free N_d phase (black circles), the nematic gel (N_d phase gelled with 2 wt% DBC, red squares) and the binary gel (H_2O gelled with 0.5 wt% DBC, blue triangles), obtained via oscillation frequency (ω) sweeps at constant shear stress and temperature.

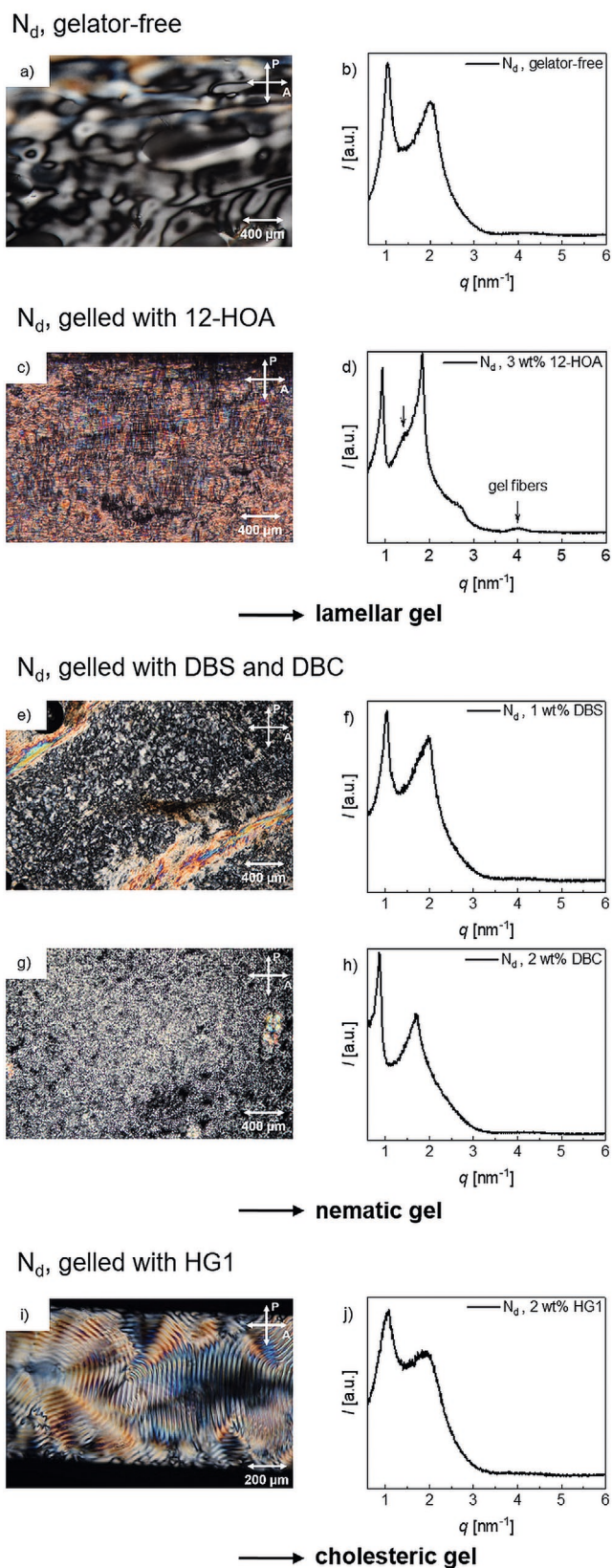


Figure 2. a–j) Comparison of the gelator-free N_d phase with the N_d phase gelled with the different LMWGs. (left) POM images of the gelator-free N_d phase (a) and of the gels obtained with 12-HOA (c), DBS (e), DBC (g), and HG1 (i). (right) X-ray diffraction profiles of the gelator-free N_d phase (b) and of the gels obtained with 12-HOA (d), DBS (f), DBC (h), and HG1 (j). Gelation of the lyotropic nematic N_d phase with the gelator 12-HOA leads to a lamellar gel. Contrary, gelation of the N_d phase with the LMWGs DBS and DBC results in a nematic gel. When using HG1 to gel the N_d phase, the formation of a chiral nematic gel is observed. The layered structure of the 12-HOA fibers^[55,56] reveals itself by two small and broad maxima at $q = 1.35 \text{ nm}^{-1}$ and $q = 4.04 \text{ nm}^{-1}$. Contrary, the presence of gel fibers of DBS, DBC, and HG1 is not reflected in the X-ray profiles.

significantly influences its gelling properties since 12-HOA is partly incorporated into the micelles, acting as a cosurfactant and thus reducing the micelle curvature. As a result, the nematic phase is transferred into a lamellar gel, as proven by POM and X-ray investigations.^[40] The challenge is thus to find gelators that are not incorporated into the micelles and leave the LLC phase unchanged upon gelation.

In fact, gelation of the N_d phase with DBS and DBC successfully leads to nematic gels, as proven by the schlieren textures observed in POM examinations and X-ray profiles that resemble the one of the gelator-free N_d phase (see Figure 2e–h). In all cases, a relatively sharp first order and a diffuse second order scattering maxima are observed indicating the presence of a pseudo-lamellar structure. The peak shape analysis (Figure S9 and Table S3, Supporting Information) reveals that the correlation length is about 150 Å and remains practically in the same range for the gelled N_d phases. The SAXS study thus demonstrates that the nematic structure remains essentially unchanged in the gelled state and a comparison with the X-ray profile of a L_α phase (Figure 2d), which exhibits significantly sharper peaks confirms the nematic nature of all samples.

The X-ray curve of the N_d phase gelled with HG1 also clearly proves the absence of translational order, but the POM image reveals a fingerprint texture, typical of a chiral nematic phase (see Figure 2j). Obviously, gelation of the N_d phase with HG1 leads to a lyotropic cholesteric gel, due to (heterogeneous) chiral induction by the twisted gel fibers.

To gain further insights into the structure of the lyotropic nematic gels we performed 2D small angle X-ray scattering (2D SAXS). In many cases, a uniform director configuration is observed (Figure 3). Even though the gel fiber network forms first, not a nematic polydomain structure (as sketched in Figure 1b) but a macroscopically aligned nematic gel is obtained. We assume that in thin capillaries (700 μm) the fibers grow along the capillary axis and thus the director of the N_d phase is aligned perpendicular to it. Like in other types of anisotropic hydrogels^[22,31,50] and LCEs,^[51–53] such monodomains of lyotropic nematic networks are essential, for the potential use of LLC gels as actuators and sensors. However, a director alignment as shown in Figure 3b is not always reproducible. In some cases, nematic polydomain gels were observed as well. Similar investigations on the N_c phase gelled with DBS, DBC and HG1 are found in the Supporting Information.

In conclusion, we have shown that anisotropic hydrogels are available relatively easy by gelling micellar lyotropic nematic host phases with gelators which do not have an amphiphilic structure and thus do not act as a cosurfactant. In certain cases, a chirality transfer from the helical gel fibers to the LC phase might also result in cholesteric gels. Similar to their

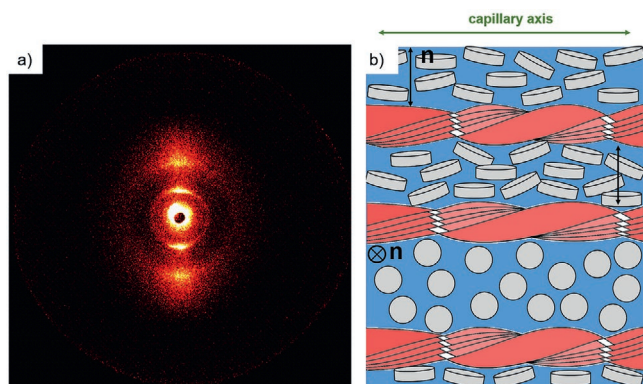


Figure 3. a) 2D SAXS diffractogram of the N_d phase gelled with 2 wt% DBC. Although the gel fibers form first, an oriented director configuration is observed. Probably, the capillary surface guides a linear growth of the gel fibers which in turn serve as a soft template for the N_d phase, as shown in (b), the schematic drawing of the gelled N_d phase.

thermotropic counterparts (LCEs), micellar lyotropic nematic gels are most interesting as stimuli-responsive water-based systems for applications in sensing and actuation.

Experimental Section

Sample Preparation: The lyotropic nematic phases N_d and N_c of the ternary system sodium dodecylsulfate (SDS, SigmaAldrich, BioUltra, $\geq 99\%$) as surfactant, *n*-decanol (DOH, Merck, $\geq 99\%$) as co-surfactant and bidistilled water, as well as of a second ternary system containing *N,N*-dimethyl-*N*-ethylhexadecylammonium bromide (CDEAB, Merck, $> 98\%$) as surfactant, DOH as cosurfactant and water were studied. To transfer the nematic phases into the gel state the LMWGs 1,3:2,4-dibenzylidene-*D*-sorbitol (DBS, NJC Europe), *N,N'*-dibenzoyl-L-cystine (DBC, Santa Cruz) and the tris-amido-cyclohexane derivative HG1 (kindly provided by the group of van Esch, TU Delft, synthesized as described in ref. [54]) were used. All chemicals were used without further purification. The nematic gels were prepared with the same water mass fraction ($\omega_{H_2O} = \frac{m_{H_2O}}{m_{tot}} = \text{const.}$) and the same cosurfactant to surfactant ratio ($\gamma = \frac{m_{\text{cosurfactant}}}{m_{\text{surfactant}}} = \text{const.}$) than the gelator-free nematic phases by adding the LMWG ($\text{wt}\%_{\text{LMWG}} = \frac{m_{\text{LMWG}}}{m_{\text{tot}}} \times 100$). Please consult the Supporting Information for the exact composition of the respective samples. The gelator-free nematic phases were prepared by weighing surfactant and water into a glass vial sealed by a screw plug and subsequent shaking of the mixture for about 1 h at 40 °C (thermoshaker Biosan, PST-60HL) until the surfactant was dissolved. DOH was added and the sample was placed on a roll mixer (Phoenix Instruments, RS-TR05) at room temperature for one day to ensure homogenization of the sample. N_d and N_c phases were differentiated by the way they attach to a polar glass surface and align in a magnetic field (see Figures S2 and S3, Supporting Information). To obtain nematic gels the proper amount of LMWG was added to the sample and dissolved by heating the sample up in a thermoshaker (Hettich, MHR-23, 95 °C, 500 rpm, 10 min). Afterward, the sample was kept at room temperature for one day until gelation was completed. Samples were considered gelled when no flow occurred in an inverted vessel for at least 8 h. Please consult Table S1 in the Supporting Information for the respective critical gelation concentrations (cgc), which is for a given sample the minimal gelator concentration necessary to obtain a gel.

Methods: Polarizing microscopy was performed at room temperature using a Leica DMLP polarizing microscope. Photographs of the textures were taken by a Nikon D5300 camera. Samples were filled into flat capillaries (Camlab UK) with a cross-section of 0.3 mm \times 3 mm

and were flame sealed. 1D small-angle X-ray studies were carried out with a SAXSess system (Anton Paar). The X-ray radiation (Cu- K_{α} , $\lambda = 0.15418$ nm) was generated by an ISO-DEBYEFLEX 3003 X-ray generator (GE Inspection Technologies GmbH) and the X-ray scattering was recorded using a CMOS detector (Dectris, Mythen 2 1K). Temperature was controlled by the sample holder unit TSC 120. 2D small angle X-ray scattering was carried out on a Bruker AXS Nanostar X-ray diffractometer (Cu- K_{α} radiation, $\lambda = 0.15418$ nm, generated by a Kristalloflex 770 generator, 100 μm point-collimated X-ray beam, 60 cm sample to detector distance, VÁNTEC 500 2D digital Mikrogap area detector and a home-built temperature-controlled sample holder with a magnetic field of 0.7 T). Samples were filled into Mark capillary tubes (Hilgenberg, glass No. 14) with an outer diameter of 0.7 mm and a wall thickness of 0.01 mm. Freeze fracture electron microscopy replicas of the gelled samples were prepared with the freeze fracture and etching system EM BAF060 from Leica. After quenching the sample in liquid ethane and fracturing it, the surface was replicated by a layer of Pt/C (≈ 2 nm) deposited at an angle of 45° and stabilized by a layer of pure carbon (≈ 20 nm) at 90° in the vacuum chamber of the BAF060 at -150 °C. The replicas were examined using a transmission electron microscope EM10 from Zeiss operated at 60 kV. Oscillating shear rheometry was measured using a Physica MCR 501 (Anton Paar) rheometer with a plate-plate geometry (diameter of upper plate 25 mm) and a constant gap size of 1 mm. For all measurements, temperature was set to 24 °C and water evaporation reduced by a solvent gap. To determine the limit of the linear viscoelastic range first amplitude sweeps at a constant angular frequency of $\omega = 10$ s $^{-1}$ and an increasing shear stress τ were carried out. Oscillation frequency sweeps were then executed at an appropriate constant shear stress ($\tau = 2$ Pa for the gelator-free N_d phase and $\tau = 40$ Pa for the gelled N_d phase and the binary gel) varying the angular frequency ω from 100 to 0.05 s $^{-1}$.

Supporting Information

Supporting Information is available from the Wiley Online Library or from the author.

Acknowledgements

The authors gratefully acknowledge financial support from the Deutsche Forschungsgemeinschaft (DFG Gi-243/9-1) and Fonds der Chemischen Industrie (FCI). The authors thank Tabea Pfister for the preparation of the samples studied in Figure S3 (Supporting Information). Many thanks to Ke Peng for the introduction into the rheometer.

Open access funding enabled and organized by Projekt DEAL.

Conflict of Interest

The authors declare no conflict of interest.

Keywords

low-molecular-weight gelators, lyotropic liquid crystals, lyotropic nematic gels, self-assembled fibrillar networks

Received: October 27, 2020

Revised: December 7, 2020

Published online: January 18, 2021

[1] P.-G. de Gennes, M. Hébert, R. Kant, *Macromol. Symp.* **1997**, 113, 39.

- [2] M.-H. Li, P. Keller, *Philos. Trans. R. Soc., A* **2006**, 364, 2763.
- [3] F. J. Davis, *J. Mater. Chem.* **1993**, 3, 551.
- [4] S. Mayer, R. Zentel, *Curr. Opin. Solid State Mater. Sci.* **2002**, 6, 545.
- [5] T. J. White, D. J. Broer, *Nat. Mater.* **2015**, 14, 1087.
- [6] T. Kato, T. Kutsuna, K. Hanabusa, M. Ukon, *Adv. Mater.* **1998**, 10, 606.
- [7] L. Guan, Y. Zhao, *J. Mater. Chem.* **2001**, 11, 1339.
- [8] T. Kato, Y. Hirai, S. Nakaso, M. Moriyama, *Chem. Soc. Rev.* **2007**, 36, 1857.
- [9] E.-K. Fleischmann, H.-L. Liang, N. Kapernaum, F. Giesselmann, J. Lagerwall, R. Zentel, *Nat. Commun.* **2012**, 3, 1178.
- [10] M. Rogó z, H. Zeng, C. Xuan, D. S. Wiersma, P. Wasylczyk, *Adv. Opt. Mater.* **2016**, 4, 1689.
- [11] S. Schuhladen, F. Preller, R. Rix, S. Petsch, R. Zentel, H. Zappe, *Adv. Mater.* **2014**, 26, 7247.
- [12] M.-H. Li, P. Keller, J. Yang, P.-A. Albouy, *Adv. Mater.* **2004**, 16, 1922.
- [13] M. Camacho-Lopez, H. Finkelmann, P. Palffy-Muhoray, M. Shelley, *Nat. Mater.* **2004**, 3, 307.
- [14] J. M. McCracken, B. R. Donovan, T. J. White, *Adv. Mater.* **2020**, 32, 1906564.
- [15] K. Sano, Y. Ishida, T. Aida, *Angew. Chem., Int. Ed.* **2018**, 57, 2532.
- [16] S. A. Willis, G. R. Dennis, G. Zheng, W. S. Price, *React. Funct. Polym.* **2013**, 73, 911.
- [17] F. A. Aouada, M. R. de Moura, P. R. G. Fernandes, A. F. Rubira, E. C. Muniz, *Eur. Polym. J.* **2005**, 41, 2134.
- [18] C. L. Lester, S. M. Smith, C. D. Colson, C. A. Guymon, *Chem. Mater.* **2003**, 15, 3376.
- [19] M. Hayakawa, T. Onda, T. Tanaka, K. Tsujii, *Langmuir* **1997**, 13, 3595.
- [20] F. Kleinschmidt, M. Hickl, K. Saalw chter, C. Schmidt, H. Finkelmann, *Macromolecules* **2005**, 38, 9772.
- [21] C.  zdilek, E. Mendes, S. J. Picken, *Polymer* **2006**, 47, 2189.
- [22] N. Miyamoto, M. Shintate, S. Ikeda, Y. Hoshida, Y. Yamauchi, R. Motokawa, M. Annaka, *Chem. Commun.* **2013**, 49, 1082.
- [23] A. F. Mejia, R. Ng, P. Nguyen, M. Shuai, H. Y. Acosta, M. S. Mannan, Z. Cheng, *Soft Matter* **2013**, 9, 10257.
- [24] L. Chen, Q. Wu, J. Zhang, T. Zhao, X. Jin, M. Liu, *Polymer* **2020**, 192, 122309.
- [25] Z. Zhu, G. Song, J. Liu, P. G. Whitten, L. Liu, H. Wang, *Langmuir* **2014**, 30, 14648.
- [26] M. F. Islam, A. M. Alsayed, Z. Dogic, J. Zhang, T. C. Lubensky, A. G. Yodh, *Phys. Rev. Lett.* **2004**, 92, 88303.
- [27] D. J. Abdallah, R. G. Weiss, *Adv. Mater.* **2000**, 12, 1237.
- [28] X. Du, J. Zhou, J. Shi, B. Xu, *Chem. Rev.* **2015**, 115, 13165.
- [29] M. George, R. G. Weiss, *Acc. Chem. Res.* **2006**, 39, 489.
- [30] L. E. Buerkle, S. J. Rowan, *Chem. Soc. Rev.* **2012**, 41, 6089.
- [31] L. E. Millon, H. Mohammadi, W. K. Wan, *J. Biomed. Mater. Res., Part B* **2006**, 79, 305.
- [32] D.-H. Kim, A. Jahn, S.-J. Cho, J. S. Kim, M.-H. Ki, D.-D. Kim, *J. Pharm. Invest.* **2015**, 45, 1.
- [33] L. Kang, H. H. Cheong, S. Y. Chan, P. F. C. Lim, in *Soft Fibrillar Materials: Fabrication and Applications* (Eds: X. Y. Liu, J.-L. Li), Wiley-VCH, Weinheim, Germany **2013**, pp. 115–128.
- [34] C. Wang, D. Chen, X. Jiao, *Sci. Technol. Adv. Mater.* **2009**, 10, 023001.
- [35] S. H. Tolbert, A. Firouzi, G. D. Stucky, B. F. Chmelka, *Science* **1997**, 278, 264.
- [36] Y. Xu, M. Laupheimer, N. Preisig, T. Sottmann, C. Schmidt, C. Stubenrauch, *Langmuir* **2015**, 31, 8589.
- [37] S. Koitani, S. Dieterich, N. Preisig, K. Aramaki, C. Stubenrauch, *Langmuir* **2017**, 33, 12171.
- [38] K. Steck, C. Stubenrauch, *Langmuir* **2019**, 35, 17132.
- [39] K. Steck, N. Preisig, C. Stubenrauch, *Langmuir* **2019**, 35, 17142.
- [40] S. Dieterich, T. Sottmann, F. Giesselmann, *Langmuir* **2019**, 35, 16793.
- [41] E. Akpınar, C. Canioz, M. Turkmen, D. Reis, A. M. Figueiredo Neto, *Liq. Cryst.* **2018**, 45, 219.
- [42] E. Akpınar, K. Otluo lu, M. Turkmen, C. Canioz, D. Reis, A. M. Figueiredo Neto, *Liq. Cryst.* **2016**, 43, 1693.
- [43] E. Akpınar, M. Turkmen, C. Canioz, A. M. F. Neto, *Eur. Phys. J. E: Soft Matter Biol. Phys.* **2016**, 39, 107.
- [44] D. Zhang, Q. Liu, R. Visvanathan, M. R. Tuchband, G. H. Sheetah, B. D. Fairbanks, N. A. Clark, I. I. Smalyukh, C. N. Bowman, *Soft Matter* **2018**, 14, 7045.
- [45] P. Terech, *Liq. Cryst.* **2006**, 9, 59.
- [46] B. J. Lemaire, P. Panine, J. C. P. Gabriel, P. Davidson, *Europhys. Lett.* **2002**, 59, 55.
- [47] J. Campbell, M. Kuzma, M. M. Labes, *Mol. Cryst. Liq. Cryst.* **2011**, 95, 45.
- [48] H. C. Yun, E. Y. Chu, Y. K. Han, J. L. Lee, T. K. Kwei, Y. Okamoto, *Macromolecules* **1997**, 30, 2185.
- [49] J. B. Jones, C. R. Safinya, *Biophys. J.* **2008**, 95, 823.
- [50] R. M. Erb, J. S. Sander, R. Grisch, A. R. Studart, *Nat. Commun.* **2013**, 4, 1712.
- [51] O. M. Wani, H. Zeng, A. Priimagi, *Nat. Commun.* **2017**, 8, 15546.
- [52] D. L. Thomsen, P. Keller, J. Naciri, R. Pink, H. Jeon, D. Shenoy, B. R. Ratna, *Macromolecules* **2001**, 34, 5868.
- [53] C. Ohm, M. Brehmer, R. Zentel, *Adv. Mater.* **2010**, 22, 3366.
- [54] K. J. C. van Bommel, C. van der Pol, I. Muizebelt, A. Friggeri, A. Heeres, A. Meetsma, B. L. Feringa, J. van Esch, *Angew. Chem., Int. Ed.* **2004**, 43, 1663.
- [55] T. Tachibana, T. Mori, K. Hori, *Bull. Chem. Soc. Jpn.* **1980**, 53, 1714.
- [56] P. Terech, *Colloid Polym. Sci.* **1991**, 269, 490.